JPE 8-2-6

Cost-Effective Converters for Micro Wind Turbine Systems using PMSG

Hong-Geuk Park*, Dong-Choon Lee† and Heung-Geun Kim**

†*Dept. of Electrical Eng., Yeungnam University, Gyeongsan , Korea
**School of Electrical Eng. and Computer Science, Kyungpook Nat. University, Daegu, Korea

ABSTRACT

This paper proposes a low-cost power converter for micro wind turbine systems using permanent magnet synchronous generators (PMSG). The proposed converter consists of a two-leg three-phase PWM inverter for the generator control and a single-phase half-bridge PWM converter which is connected to the utility grid. For the two separate DC-link voltages, a balancing control is added and the adverse effect of the DC-link voltage ripples on the inverter output voltage is compensated. The control performance of the proposed converter topology for the micro wind turbine system is shown by the simulation results using PSIM software.

Keywords: Low-cost converter, Micro wind turbine, Permanent magnet synchronous generator

1. Introduction

In recent years, development of renewable energy systems is rapidly increasing since the crisis of the exhaustion of fossil fuel and environmental pollution are hot issues. Among different types of renewable energy, wind power is the most promising and widely commercialized compared with other energy sources. The trend of the wind power system is to employ large wind turbine systems, such as multi-mega watt power capacity (3~5[MW]), and to construct the large wind farms[1]. However, micro wind turbine systems can be used for islands, mountains, and local areas which are isolated from the utility grid. The small-power wind turbine system is also a good candidate for the microgrid systems[2].

Manuscript received Jan. 23, 2008; revised Feb. 18, 2008
† Corresponding Author: dclee@yu.ac.kr
Tel: +82-53-8102582, Fax: +82-53-8104767, Yeungnam Univ.
*Dept. of Electrical Eng., Yeungnam University, Korea
**School of Electrical Eng. and Computer Science, Kyungpook Nat. University, Korea

For MPPT (maximum power point tracking) control of the turbine system, some methods have been used. One is P&O (perturbation and observation) which controls the output power to maximum by changing the rotational speed in steps[3]. Another method is to use the optimal tip-speed ratio which produces the turbine (or generator) speed reference according to the wind speed[4]. A third method is to use the torque control which gives the maximum output power for the given rotational speed[5].

The conventional power converter for the small power wind turbine system is shown in Fig. 1. It consists of the diode rectifier, DC-boost converter, and full-bridge PWM converter, which is of cheap structure. Since the uncontrolled diode rectifier is connected to the PMSG, it is impossible to directly control the generator speed for output power control. Input current reference of the DC-boost converter is decided for the MPPT control of the turbine[6]-[8].

In this paper, a low-cost, and high-performance converter for small-scale PMSG wind turbine systems is

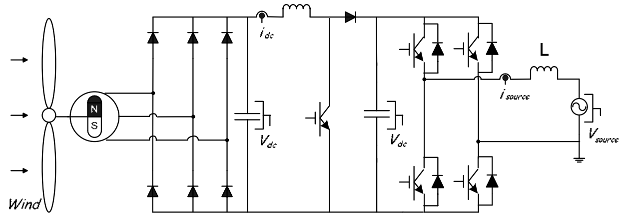

Fig. 1 Conventional small-scale wind generation system

proposed, which consists of a three-phase two-leg PWM inverter for the generator control and a single-phase half-bridge PWM converter connected to the utility grid. With this topology, vector control of the PMSG is possible, so the dynamic control performance is fast. The operation of the proposed circuit topology is shown by simulation for 3[kW] PMSG using PSIM.

2. Wind Turbine Model

The power captured by the wind turbine may be written as[9][10]

$$P_{Turbine} = 0.5 A \rho C_p(\lambda) \upsilon^3 [W] \tag{1}$$

and the tip-speed ratio is defined as

$$\lambda = \frac{\omega_r R}{\upsilon} \tag{2}$$

where,

A :blade swept area [m^2]
ρ :specific density of air [kg/m^3]
υ :wind speed [m/s]
R : radius of the turbine blade[m]
ω_r : rotating speed [rpm]
C_p : coefficient of power conversion

If the blade swept area and the air density are constant, the value of C_p is a function of λ and it is at its maximum at the particular λ_{opt}. Hence, to fully utilize the wind energy, λ should be maintained at λ_{opt}, which is determined from the blade design. Then, from (1),

$$P_{max} = 0.5 A \rho C_{pmax} \upsilon^3 [W] \tag{3}$$

The reference speed of the generator is determined from (2) as

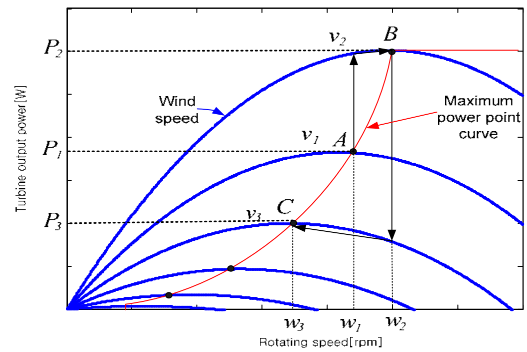

Fig. 2 Wind turbine output characteristics

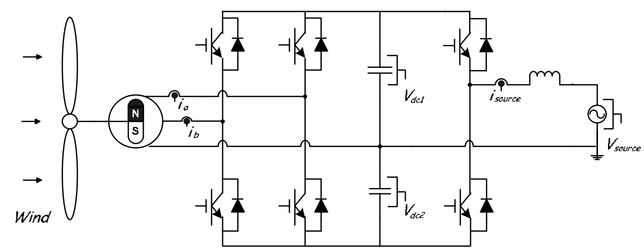

Fig. 3 Proposed converter system

Table 1 Comparison of converter topologies

Components	Converter in Fig. 1	Converter In Fig. 3
Switch(IGBT)	5	6
Diode	11	6
DC capacitor	2	2
Inductor	2	1
Voltage sensor	3	3
Current sensor	2	3

$$\omega_r^* = \frac{\lambda_{opt}}{R} \upsilon \tag{4}$$

Once the wind velocity is measured, the speed reference for the MPPT can be obtained from (4).

Fig. 2 shows the turbine power versus the rotational speed, being the wind speed as a parameter.

3. Low-Cost Converters and Control

The proposed converter consists of the two-leg PWM inverter and the single-phase half-bridge converter as shown in Fig. 3. This type of converter has been proposed for the three-phase induction motor drives which are supplied from a single-phase utility [11]. It can be used for the three-phase PMSG to be connected to the single-phase utility grid. The comparison of the conventional converter and the proposed converter topology is given in Table 1. The proposed converter requires almost the same number of components as that of the conventional type; however, it has a lot of potential for control of the PMSG. That is, its performance is similar to that of the three-phase three-leg PWM inverter and single-phase full-bridge AC/DC PWM converter system, which is much more expensive.

3.1 Control of three-phase two-leg inverters

For the PMSG control, the three-phase voltage references from the current controller are given in a balanced set as [11]-[13] ,

$$v_{as}^* = V_m cos\omega t \tag{5}$$

$$v_{bs}^* = V_m cos(\omega t - \frac{2\pi}{3}) \tag{6}$$

$$v_{cs}^* = V_m cos(\omega t + \frac{2\pi}{3}) \tag{7}$$

The two phases of the PMSG are connected to the two legs of the inverter and the third phase is connected to the neutral point of the DC-link. The line-to-line voltage instead of the phase voltage can be used for the PWM. From (5)-(7), the two line-to-line voltage references are given by

$$v_{ac}^* = v_{as}^* - v_{cs}^* = \sqrt{3} V_m cos(\omega t - \frac{\pi}{6}) \tag{8}$$

$$v_{bc}^* = v_{bs}^* - v_{cs}^* = \sqrt{3} V_m cos(\omega t - \frac{\pi}{2}) \tag{9}$$

Using the proportionality of the triangle as shown in Fig. 4, the switching time can be calculated as

$$T_1 = \frac{T_s}{2} + \frac{v_{ac}^*}{v_{dc}} T_s \tag{10}$$

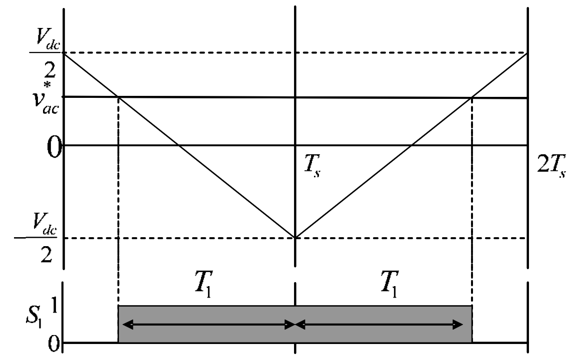

Fig. 4 Voltage modulation

$$T_2 = \frac{T_s}{2} + \frac{v_{bc}^*}{v_{dc}} T_s \tag{11}$$

where,

v_{ac}^*, v_{bc}^* : line-to-line voltage reference

T_s : sampling period

T_1, T_2 : switching time

If there is a difference between the two DC-link voltages of the upper and lower parts, which is usual because of the difference of the instantaneous waveforms, a distortion of the inverter output voltage will be made. The deterioration of waveform can be reduced by compensating for effects of the DC-link voltage ripples.

Using the compensation voltage, the switching times in (10) and (11) are modified as

$$T_1' = \frac{T_s}{2} + \frac{v_{ac}^* - v_{comp}}{v_{dc}} T_s \tag{12}$$

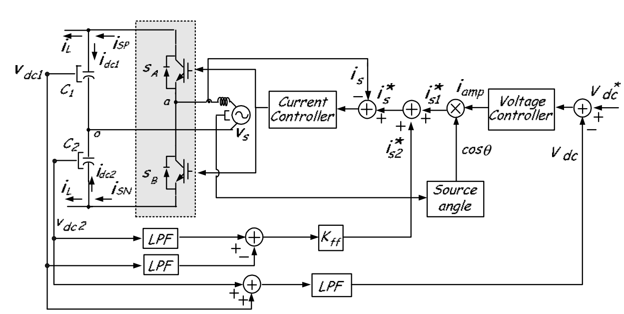

Fig. 5 Control block diagram of the grid side converter

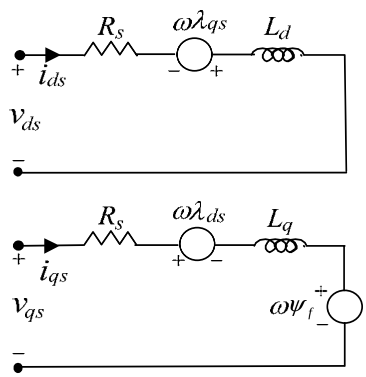

Fig. 6 D-q equivalent circuits of PMSG

$$T_2' = \frac{T_s}{2} + \frac{v_{bc}^* - v_{comp}}{v_{dc}} T_s \tag{13}$$

where

$$v_{comp} = \frac{v_{dc1} - v_{dc2}}{2}$$

3.2 Control of single-phase half-bridge rectifiers

Fig. 5 shows the control block diagram for a half-bridge PWM rectifier. For controlling the source current and the DC-link voltage, the PI regulators are employed. The source voltage angle is measured for unity power factor control. For a balancing control of the neutral voltage of the DC-link, the difference of v_{dc1} and v_{dc2} is fed back to the current controller through the proportional gain of K_{ff} . For the DC-link voltage feedback, a cut-off frequency of the low pass filter has been chosen as 50[Hz] and for the balancing control loop as 1[Hz].

4. Control of PMSG

4.1 PMSG modeling

Fig. 6 shows the d-q equivalent circuits of the PMSG. The voltage equation of the PMSG is expressed at synchronous reference frame [14] ,

$$\begin{bmatrix} v_{ds} \\ v_{qs} \end{bmatrix} = \begin{bmatrix} R_s + pL_d & -\omega_r L_q \\ \omega_r L_d & R_s + pL_q \end{bmatrix} \begin{bmatrix} i_{ds}^e \\ i_{qs}^e \end{bmatrix} + \begin{bmatrix} 0 \\ \omega_r \psi_f \end{bmatrix} \tag{14}$$

Where

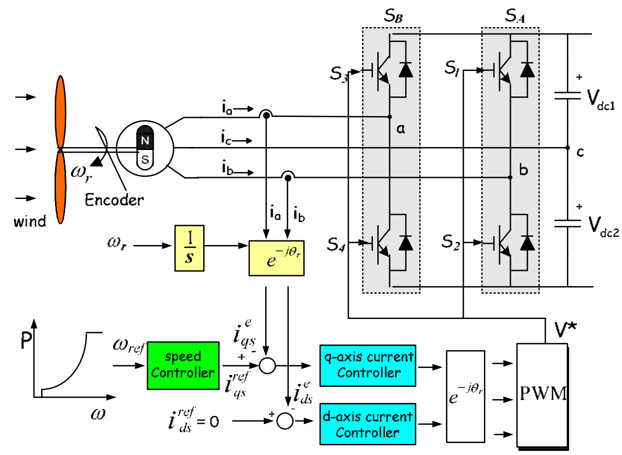

Fig. 7 Control block diagram of PMSG

p	: differential operator
v_{ds}, v_{qs}	: d-q axis stator voltage
i_{ds}^e, i_{qs}^e	: d-q axis stator current
L_d, L_q	: d-q axis inductance
R_S	: stator resistance
ω_r	: generator speed
ψ_f	: magnetic flux leakage

The electromagnetic torque is expressed as

$$T_e = \frac{3}{2}\frac{P}{2}[(L_d - L_q) i_{ds}^e i_{qs}^e + \psi_f i_{qs}^e] \tag{15}$$

where

P : number of poles

If the d-axis is aligned with the magnetic flux, then

$$T_e = \frac{3}{2}\frac{P}{2}\psi_f i_{qs}^e \tag{16}$$

The q-axis current component can be used for the speed control of the generator, and the d-axis current is controlled to be zero.

4.2 MPPT method

For MPPT control of the wind turbine system, the optimal tip-speed method is used, where wind speed information is required.

In Fig. 2, the operating point is A(P_1, w_1) at wind speed of v_1. When the wind speed is changed to v_2, the generator speed is increased to w_2, which gives the maximum power P_2. When the wind speed is changed to v_3, then the generator speed is decreased to w_3 which gives the output power P_3. In this way, the MPPT control is performed for wind speed variations.

For higher wind speeds than the rated value, the turbine power is limited by a furling for protection of the system. Thus, the machine torque and speed can be limited.

Fig. 7 shows the control block diagram of the PMSG for MPPT control.

5. Simulation Results

Simulation has been carried out to test the performance of the proposed converter topology using PSIM. The parameters of the PMSG and the turbine model are listed in Table 2 and 3, respectively, in the Appendix. The switching frequency is 5[kHz], the input boost inductor is 3[mH], the DC-link capacitor is 1,650[μF], the AC input voltage is 110[V], and the DC-link voltage is controlled to 540[V].

Fig. 8 shows the turbine and generator performance at a variable wind speed. The rated wind speed is 13[m/sec], above which it is assumed that the stall control is activated so that the turbine speed is limited at the rated value and the turbine output power is limited at 3[kW] as shown in

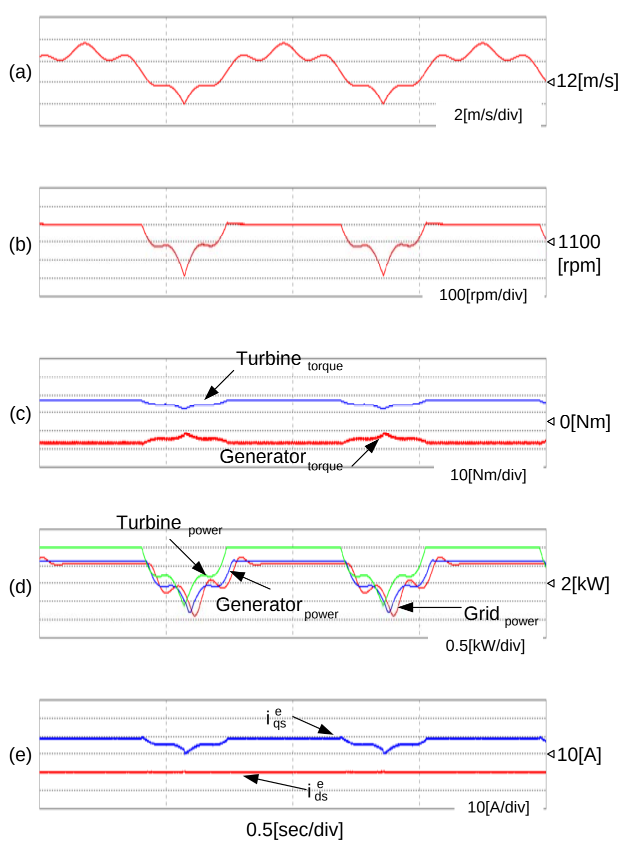

Fig. 8 Turbine and generator performance
(a) Wind speed
(b) Generator speed
(c) Turbine and generator torque
(d) Turbine, generator and grid power
(e) Dq-axis currents

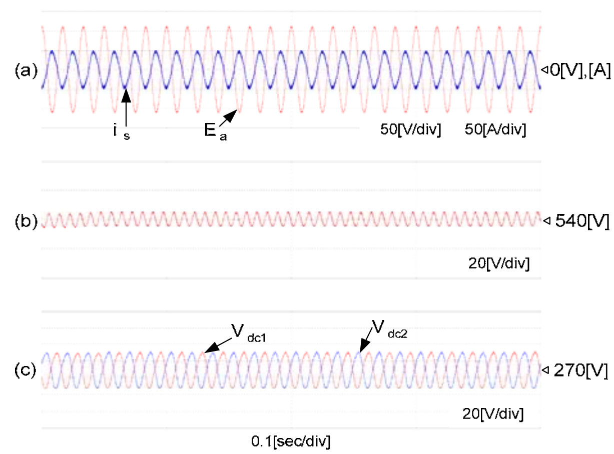

Fig. 9 Converter control performance in steady state
(a) Grid voltage and current
(b) DC-link voltage
(c) v_{dc1} and v_{dc2}

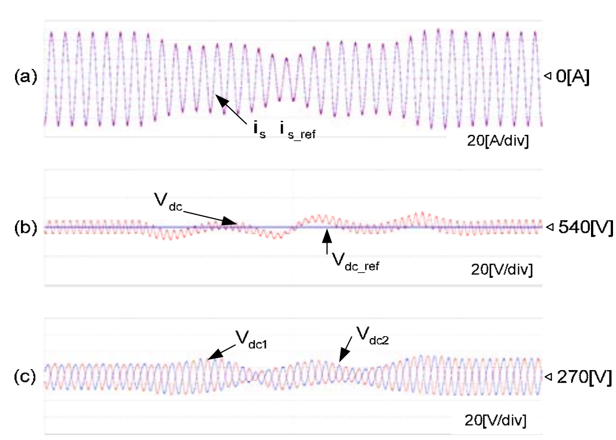

Fig. 10 Converter control performance in transient state
(a) Grid current(i_s, i_{s_ref})
(b) DC-link voltage
(c) v_{dc1} and v_{dc2}

Table 2 Ratings and parameters of PMSG

Parameters	Value
Rated power	3[kW]
Rated line voltage	220[V]
Stator resistance	0.49[Ω]
Inductance	5.35[mH]
Torque constant	2.4[Nm/A]
Back-emf constant	147[V/krpm]
Number of poles	6
Rated frequency	60[Hz]
Generator efficiency	87.3%

Parameters	Value
Blade radius	1.26 [m]
Max. power conv. coeff.	0.45
Optimal tip-speed ratio	7
Cut-in speed	3 [m/s]
Rated wind speed	13 [m/s]
Gear ratio	1

(d). At this condition, the generator output power is about 2,600[W] where the generator efficiency is 87%. The turbine generator and torques are shown in (c) with an opposite sign. It is seen in (d) that the grid power is a little delayed from the generator power due to the control performance of the converter. Fig. 8(e) shows the dq-axis currents of the generator where the d-axis current is controlled to be constant.

Fig. 9 shows the converter control performance in steady state. The grid voltage is in opposite phase with the current as shown in (a). The full DC-link voltage and each half-part of the DC-link voltage are shown in (b) and (c), respectively. Due to the ripple compensation effect of the v_{dc1} and v_{dc2}, the ripple component of the full DC-link voltage has been reduced significantly.

Fig. 10 shows the converter control performance in transient state of wind speed variations. According to the machine speed, the grid current is fluctuated and the DC-link voltages oscillate a little. However, this voltage oscillation has no effect on the generator performance.

6. Conclusions

This paper has proposed a cost-effective converter for small-scaled wind power generation systems, which consists of a two-leg three-phase PWM inverter and a half-bridge single-phase AC/DC converter. With this topology of the converter, the PMSG can be controlled in vector control mode and can give, in a fast MPPT control performance, at variable wind speeds. The validity of the proposed converter system has been verified by simulation results using the PMSG.

Appendix

The parameters of the 3[kW] PMSG and turbine model are listed in Table 2 and 3, respectively.

References

[1] American public power association, Utility wind integration state of art, Annual Report, Available: http://www.uwig.org.

[2] C. A. Hernandez-Aramburo, T. C. Green. and N. Mugniot, “Fuel consumption minimization of a microgrid”, IEEE Trans. on Industry Application, Vol. 41, No. 3, pp. 673-681, May-June 2005.

[3] R. Datta, and V. T. Ranganathan, “A method of tracking the peak power points for a variable speed wind energy conversion system”, IEEE Trans. on Energy Conversion, Vol. 18, No. 1, pp.163-168, March 2003.

[4] A. Abo-Khalil, D.-C. Lee, and S.-H. Lee, “Synchronization of DFIG output voltage to utility grid in wind power system”, IASTED Conf Proc. in Rhodes, pp.372-377, June 2006.

[5] A. Mirecki, X. Roboam, F. Richardeau, “Architecture complexity and energy efficiency of small wind turbines”, IEEE Trans. on Industrial Electronics, Vol. 54, No. 1, pp. 660-670, Feb. 2007.

[6] S. Jiao, G. Hunter, V. Ramsden, and D. Patterson, “Control system design for a 20kW wind turbine generator with a boost converter and battery bank load”, IEEE PESC Proc., 2001, pp. 2203-2206, 2001.

[7] Y. Higuchi, N. Yamamura, M. Ishida, and T. Hori, “An improvement of performance for small-scaled wind power generating system with permanent magnet type synchronous generator”, IEEE IECON Proc., Vol. 2, pp. 1037-1043, 2000.

[8] S.-H. Song, S.–I. Kang, and N.–K. Hahm, “Implementation and control of grid connected AC-DC-AC power converter for variable speed wind energy conversion system”, IEEE APEC Proc., Vol. 1, pp. 154-158, Feb.2003.

[9] A. Miller, E. Muljadi, and D. S. Zinger, “A variable speed wind turbine power control”, IEEE Trans. on Energy Conversion, Vol. 12, No. 2, pp. 181-186, 1997.

[10] A. B. Raju, K. Chatteriee, and B. G. Fernandes, “A simple maximum power point tracker for grid connected variable speed wind energy conversion system with reduced switch count power converters”, IEEE PESC Proc., Vol. 2, pp. 748-753, 2003.

[11] D.-C. Lee, and Y.–S. Kim, “Control of single-phase-to-three-phase AC/DC/AC PWM converters for induction motor drives”, IEEE Trans. on Industrial Electronics, Vol. 54, No. 2, pp. 797-804, 2007.

[12] P. Enjeti, and A. Rahman, “A new single phase to three phase converter with active input current shaping for low cost ac motor drives”, IEEE Trans. on Industry Application, Vol. 29, No. 4, pp. 806-813, 1993.

[13] M. B. de Rossiter, C. B. Jacobina, E. R. C. da Silva, and A. M. N. Lima, “A general PWM strategy for four-switch three-phase inverters”, IEEE Trans. on Power Electronics, Vol. 21, No. 6, pp. 1618-1627, Nov. 2006.

[14] M. Chinchilla, S. Arnaltes, and J. C. Burgos, “Control of permanent - magnet generators applied to variable-speed wind-energy systems connected to the grid”, IEEE Trans. on Energy Conversion, Vol. 21, No. 1, pp. 130-135, March 2006.

Hong-Geuk Park was born in 1980. He received his B.S degree in electrical engineering from Yeungnam University, Gyeongsan, Gyeongbuk, Korea in 2006. He is currently working toward his M.S. degree at the Power Electronics and Machine Control Laboratory in the same university. His research interests are wind power generation system and power quality control.

Dong-Choon Lee received his B.S., M.S., and Ph.D. degrees in electrical engineering from Seoul National University, Seoul, Korea, in 1985, 1987, and 1993, respectively. He was a Research Engineer with Daewoo Heavy Industry from 1987 to 1988. Since 1994, he has been a faculty member of the Department of Electrical Engineering, Yeungnam University, Gyeongbuk, Korea. As a Visiting Scholar, he joined the Power Quality Laboratory, Texas A&M University, College Station in 1998, the Electrical Drive Center, University of Nottingham, U.K. in 2001, and the Wisconsin Electric Machines & Power Electronic Consortium, University of Wisconsin, Madison in 2004. His research interests include AC machine drives, control of power converters, wind power generation, and power quality.

Heung-Geun Kim was born in Korea in 1956. He received his B.S., M.S., and Ph.D. degrees in electrical engineering from Seoul National University, Seoul, Korea in 1980, 1982, and 1988, respectively. From 1990 to 1991 he was with the Department of Electrical and Computer Engineering, University of Wisconsin, Madison, as a Visiting Scholar. Since 1984, he has been with the School of Electrical Eng. And Computer Science, Kyungpook National University, where he is currently a Professor. His research interests are power electronic control of electric machines, PV systems, and power converter circuits.